Online Appendix for: Demography-dispersal trait correlations modify the eco-evolutionary dynamics of range expansion, published in *American Naturalist*

Brad M. Ochocki

Julia B. Saltz

Tom E.X. Miller*

August 20, 2019

Department of BioSciences, Program in Ecology and Evolutionary Biology, Rice University, Houston, TX 77005

* Corresponding author; e-mail: tom.miller@rice.edu.

Online Appendix A: Additional Simulation Methods and Results

Supplemental Methods

Each generation of the simulation, individuals in the population mated, reproduced, died, and their offspring dispersed; this is similar to the laboratory-imposed life-cycle in *C. maculatus* invasion experiments (Miller and Inouye, 2013; Ochocki and Miller, 2017; Wagner et al., 2017). Because the landscape was modeled as an array of discrete patches, local interactions – including mate-finding, reproduction, and density-dependent population growth – took place at the patch-level. For mating, each individual selected one other individual in the same patch, at random (and with replacement), and received genetic information from that individual. Because individuals were modeled as hermaphrodites, all individuals were capable of acting as both male and female during reproduction. Under this mating system, each individual could contribute genetic information to multiple individuals, but could only receive genetic information from one individual. Individuals could not self-fertilize; all offspring were thus the product of two unique parents. In instances where a patch contained only one individual, that individual did not reproduce. Our model therefore includes a mate-finding Allee effect for singly-occupied patches.

Offspring inherited breeding values from their parents a_{jk} and maternal effects from their mother m_k, which were drawn from multivariate normal distributions according to Eq. 7 and 9. The expressed phenotype was also dependent on the environmental deviates e_i, drawn according to Eq. 11, and the population mean phenotypes μ^d and μ^r. As in similarly structured models of evolution during invasions, additive genetic variance is expected to decrease as the variance in breeding values among individuals decreases (Phillips, 2015). Each generation, we calculated the additive genetic covariance matrix G in each patch by calculating the variances and covariance among all breeding values in that patch. Offspring breeding values were then assigned according to Eq. 7, using the patch-estimated G matrix.

After mating, each individual reproduced following the density-dependent Beverton-Holt

model of population growth described in Eq. 3–5. We modeled invasions across a homogeneous landscape, assuming a fixed resource density of 10 beans in all patches. The carrying capacity K was therefore fixed across the landscape, but per-capita population growth varied among individuals according to Eq. 6.

After reproduction, parents senesced, marking the end of the generation; at the start of the next generation, their offspring dispersed. Thus, we modeled populations that were character-ized by discrete, non-overlaping generations. Offspring dispersed from their natal patch accord-ing to their latent dispersal phenotype λ_{ijk}, and dispersal distance was Poisson distributed, as in Eq. 1). While the Poisson distribution only generates positive values, individuals in the simula-tion could disperse either to the left or right. We simulated bi-directional dispersal by randomly multiplying an individual's Poisson distance by -1 (for leftward dispersal) or +1 (for rightward dispersal), with equal probability for each direction. After dispersal, individuals mated with an individual in the patch that they dispersed to, they reproduced, and they senesced. We simulated this process for 20 generations, on par with similar timescales of eco-evolutionary dynamics in empirical systems (Ochocki and Miller, 2017; Weiss-Lehman et al., 2017; Williams et al., 2016).

Parameter values and definitions are provided in Table A1. As described in the main text, we ran these simulations over a range of variation in trait correlations (ρ_G, ρ_M, and ρ_E) and for three cases corresponding to low (as in the beetle system), medium, and high amounts of addi-tive genetic variance, holding total phenotypic variance constant. For each case, we contrasted results against a no-evolution scenario in which the genetic variance was set to near-zero (0.001) and redistributed between maternal and environmental components. The no-evolution treatment suppressed all evolutionary processes during range expansion. We were additionally interested in isolating the role of spatial sorting, an evolutionary process unique to spraeding populations. To do so, we implemented an additional treatment for each of our parameter combinations in which the locations of all individuals were spatially shuffled following dispersal in each gen-eration. The shuffle treatment prevents dispersal genotypes from sorting along the expansion gradient but allows other evolutionary processes (natural selection) to continue to operate. Con-

trasts between control and shuffled invasions reveal the specific influence of spatial sorting.

All simulations were conducted using Julia 0.5.0 (Bezanson et al., 2017), and all analyses were conducted using R 3.4.0 (R Core Team, 2015). All code for the simulation and analyses is publicly available at `https://github.com/bochocki/correlatedtraits`.

Table A1: **Parameter values and definitions.** Descriptions of key parameters in the simulation.

Parameter	Value(s)	Definition
N_0	20	Initial population size
μ_d	1.64	Initial mean dispersal phenotype
μ_r	2.74	Initial mean fertility phenotype
$V_{P,d}$	0.384	Initial total phenotypic variance in dispersal
$V_{P,r}$	0.351	Initial total phenotypic variance in fertility
$V_{G,d}$	[0.031,0.128,0.382]	Initial genetic variance in dispersal
$V_{G,r}$	[0.033,0.117,0.349]	Initial genetic variance in fertility
$V_{M,d}$	[0.102,0.128,0.001]	Initial maternal variance in dispersal
$V_{M,r}$	[0.02,0.117,0.001]	Initial maternal variance in fertility
$V_{E,d}$	[0.251,0.128,0.001]	Initial environmental variance in dispersal
$V_{E,r}$	[0.298,0.117,0.001]	Initial environmental variance in fertility
ρ_G	[-0.9, -0.45, 0.0, 0.45, 0.9]	Additive genetic correlation
ρ_M	[-0.9, 0.0, 0.9]	Maternal correlation
ρ_E	[-0.9, 0.0, 0.9]	Environmental correlation
K	3.81	Carrying capacity per bean
Generations	20	Number of generations of invasion
Replicates	1000	Number of simulation replicates

Supplemental results and discussion

Figure A1 shows the final extent of simulated invasions subject to control (spatially sorted) conditions (A–C), shuffle treatment (D–F), and no-evolution (G–I) for each of the three cases of genetic variance (columns). In the main text, we focused on the contrast between sorted and no-evolution conditions, representing this contrast as a fold-change (Fig. 3). Here we see that increasing the genetic correlation (ρ_G) accelerated invasion not only for the spatial sorting treatment but also for the shuffle treatment, though it remained the case that sorted invasions were always faster and benfitted more from positive genetic correlations than shuffled ones. Similarly, the CV of final extent for shuffled invasions was also positively related to ρ_G, but less so than were sorted invasions (Fig. A2). These results reflect the fact that shuffled invasions were still evolving, just not by spatial sorting and its associated evolutionary mechanisms. In shuffled invasions, natural selection likely acted to favor increased fertilty, in which case positive genetic correlations would also promote greater dispersal, on average across the range – this would explain why the speed of shuffled invasions increased with ρ_G. Non-genetic correlations were completely unimportant for shuffled invasions, which was expected since the shuffle method (implemented after dispersal and before reproduction), intentionally breaks any association between location and trait values, regardless of whether that association arises by genetic or non-genetic correlations.

Range-edge trait values following invasion are shown in Fig. A3. Here we see that dispersal consistently showed a stronger evolutionary response under spatial sorting than shuffle treatment (Fig. A3A–C), as expected. Interestingly, fertility showed a different pattern (Fig. A3D–F), with sorted invasions showing greater evolved fertility than shuffle under positive genetic correlation, but lower evolved fertility than shuffle under negative genetic correlation. This likely reflects the dominant role of spatial sorting of dispersal under control conditions, which means that fertility evolution is driven primarily through its association with dispersal; this leads to strong gains in fertility under positive correlation and strong loss of fertility under negative correlation. When the force of spatial sorting is removed, fertility is more free to evolve by natural selection, leading

5

to increases over the no-evolution trait value but not reaching the strong increases seen in sorted invasions with positive trait correlation.
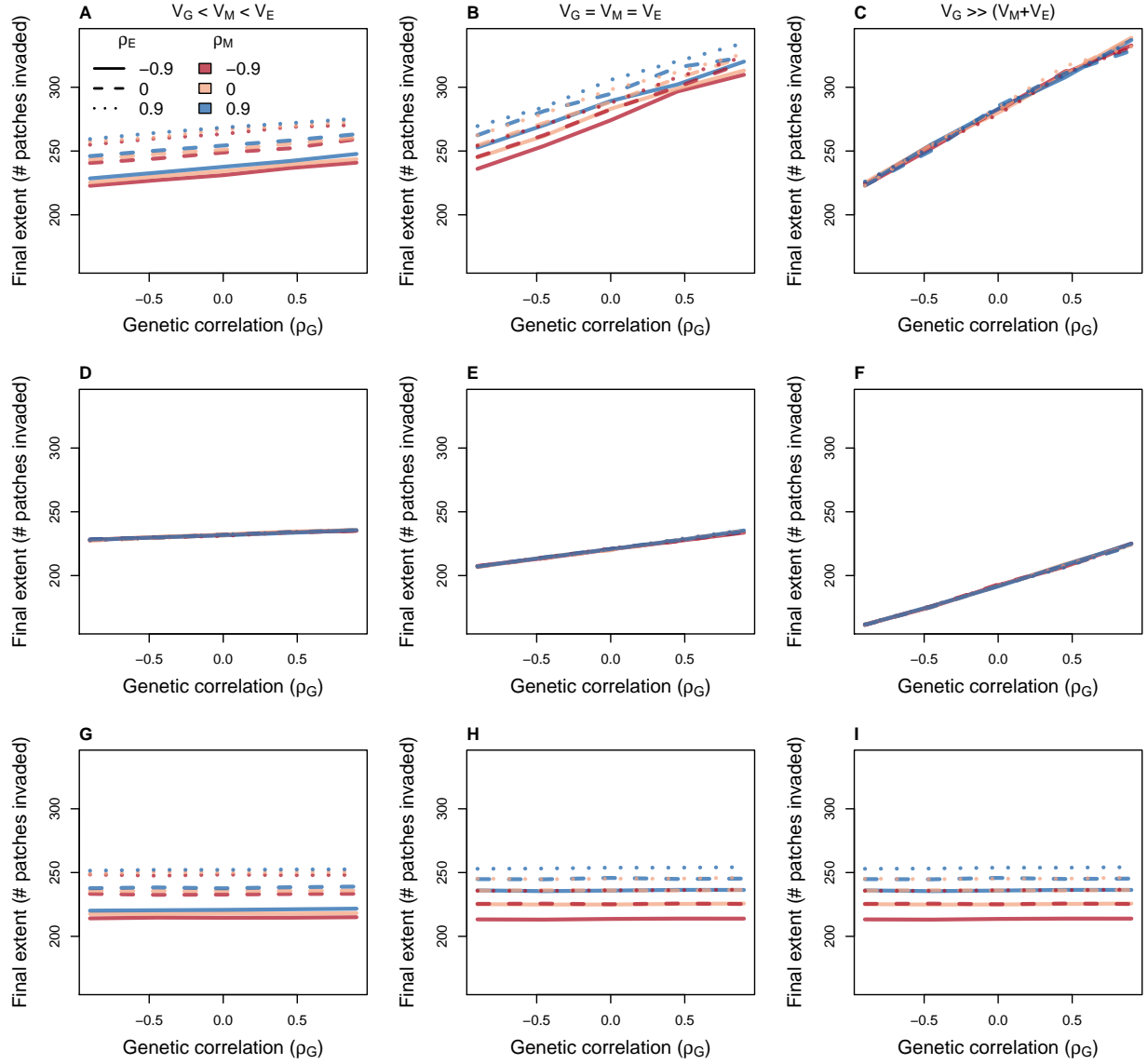
Figure A1: **Final extent of simulated invasions.** *A–C*, Control conditions subject to all evolutionary processes, including spatial sorting; *D–F*, Shuffle treatment that 'turns off' spatial sorting but maintains other, non-spatial evolutionary processes; *G–I*, No-evolution treatment, where populations had near-zero additive genetic variance in demography and dispersal traits. Columns correspond to cases of increases genetic variance in demography and dispersal, as indicated.
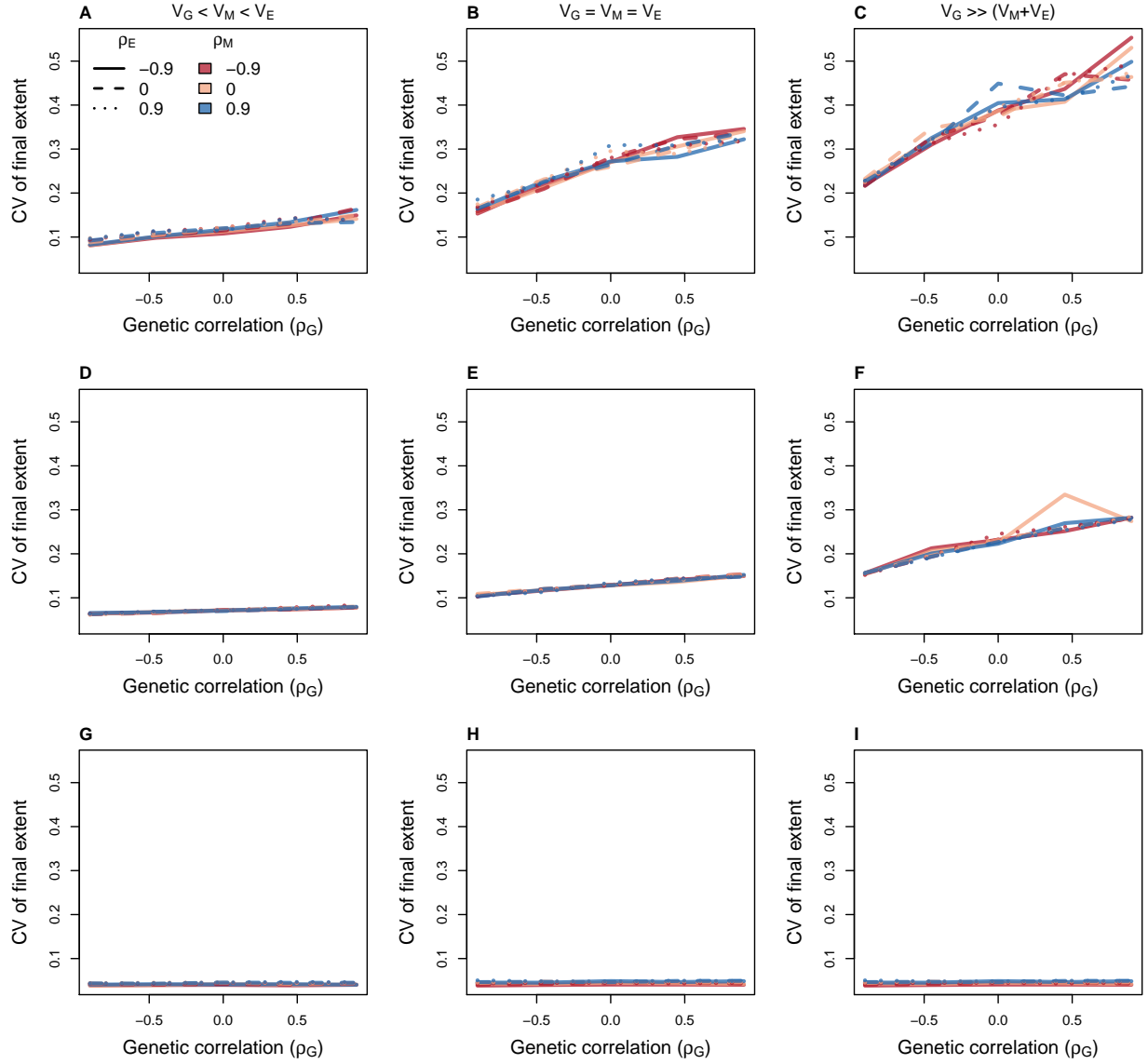
Figure A2: **CV of final extent for simulated invasions.** *A–C*, Control conditions subject to all evolutionary processes, including spatial sorting; *D–F*, Shuffle treatment that 'turns off' spatial sorting but maintains other, non-spatial evolutionary processes; *G–I*, No-evolution treatment, where populations had near-zero additive genetic variance in demography and dispersal traits. Columns correspond to cases of increases genetic variance in demography and dispersal, as indicated.
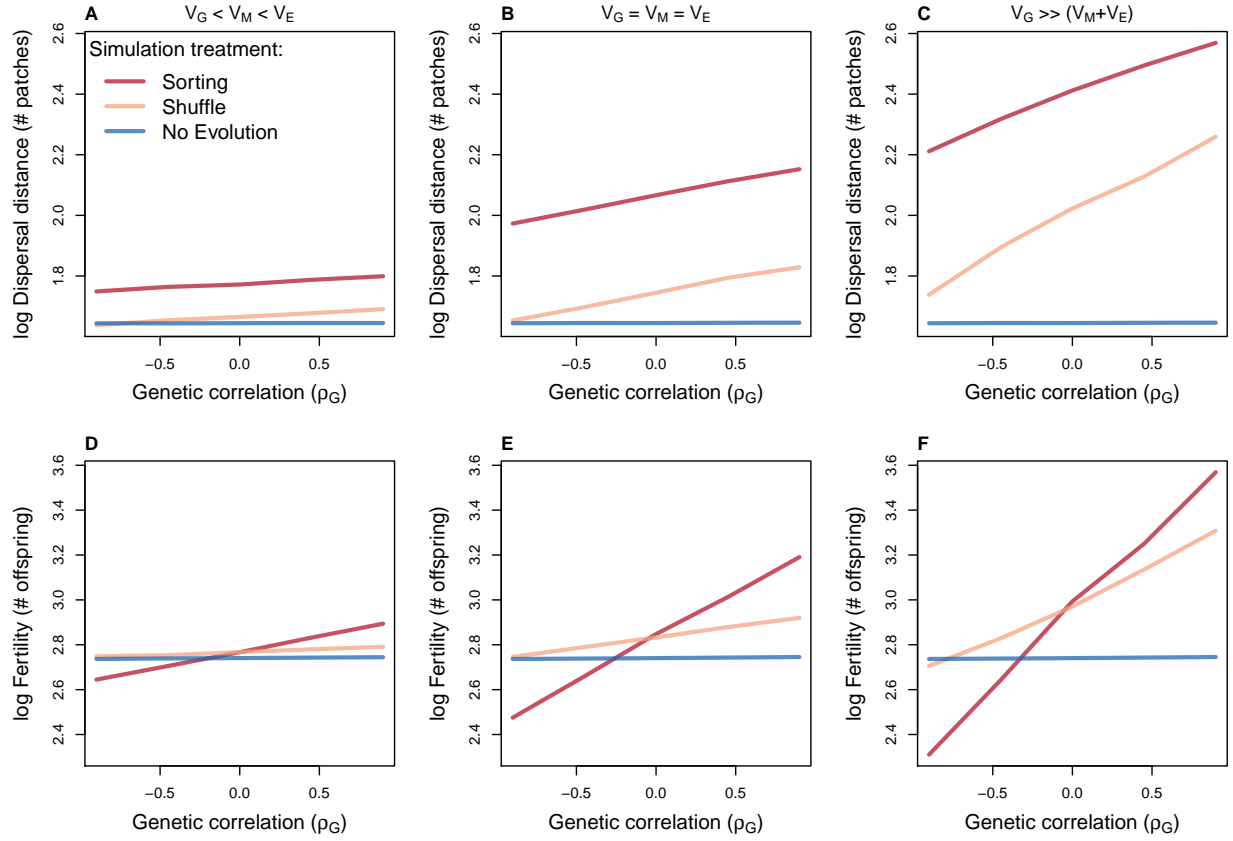
Figure A3: **Final trait values for simulated invasions.** Lines show range-edge traits values for mean dispersal distance (*A–C*) and fertility (*D–F*) after 20 generations of invasion in relation to the genetic correlation between them (ρ_G). Simulation treatments are shown as line colors and columns correspond to cases of increases genetic variance in demography and dispersal, as indicated.

Literature Cited

Bezanson, J., A. Edelman, S. Karpinski, and V. Shah. 2017. Julia: a fresh approach to numerical computing. SIAM Review 59:65–98.

Miller, T. E. X., and B. D. Inouye. 2013. Sex and stochasticity affect range expansion of experimental invasions. Ecology Letters 16:354–361.

Ochocki, B. M., and T. E. X. Miller. 2017. Rapid evolution of dispersal ability makes biological invasions faster and more variable. Nature Communications 8:14315.

Phillips, B. L. 2015. Evolutionary processes make invasion speed difficult to predict. Biological Invasions 17:1949–1960.

R Core Team. 2015. R: a language and environment for statistical computing. R Foundation for Statistical Computing, Vienna, Austria.

Wagner, N. K., B. M. Ochocki, K. M. Crawford, A. Compagnoni, and T. E. Miller. 2017. Genetic mixture of multiple source populations accelerates invasive range expansion. Journal of Animal Ecology 86:21–34.

Weiss-Lehman, C., R. A. Hufbauer, and B. A. Melbourne. 2017. Rapid trait evolution drives increased speed and variance in experimental range expansions. Nature Communications 8:14303.

Williams, J. L., B. E. Kendall, and J. M. Levine. 2016. Rapid evolution accelerates plant population spread in fragmented experimental landscapes. Science 353:482–485.